

BASIC RESEARCH PAPER

 OPEN ACCESS

## Iron-depletion promotes mitophagy to maintain mitochondrial integrity in pathogenic yeast *Candida glabrata*

Minoru Nagi<sup>a</sup>, Koichi Tanabe<sup>a,b</sup>, Hironobu Nakayama<sup>c</sup>, Keigo Ueno<sup>a</sup>, Satoshi Yamagoe<sup>a</sup>, Takashi Umeyama<sup>a</sup>, Hideaki Ohno<sup>a,d</sup>, and Yoshitsugu Miyazaki<sup>a</sup>

<sup>a</sup>Department of Chemotherapy and Mycoses, National Institute of Infectious Diseases, Shinjuku-ku, Tokyo, Japan; <sup>b</sup>Department of Food Science and Human Nutrition, Faculty of Agriculture, Ryukoku University, Otsu, Shiga, Japan; <sup>c</sup>Faculty of Pharmaceutical Sciences, Suzuka University of Medical Science, Suzuka, Mie, Japan; <sup>d</sup>Department of Infectious Diseases and Infection Control, Saitama Medical Center, Saitama Medical University, Saitama, Japan.

### ABSTRACT

*Candida glabrata*, a haploid budding yeast, is the cause of severe systemic infections in immune-compromised hosts. The amount of free iron supplied to *C. glabrata* cells during systemic infections is severely limited by iron-chelating proteins such as transferrin. Thus, the iron-deficiency response in *C. glabrata* cells is thought to play important roles in their survival inside the host's body. In this study, we found that mitophagy was induced under iron-depleted conditions, and that the disruption of a gene homologous to *ATG32*, which is responsible for mitophagy in *Saccharomyces cerevisiae*, blocked mitophagy in *C. glabrata*. The mitophagic activity in *C. glabrata* cells was not detected on short-period exposure to nitrogen-starved conditions, which is a mitophagy-inducing condition used in *S. cerevisiae*. The mitophagy-deficient *atg32Δ* mutant of *C. glabrata* also exhibited decreased longevity under iron-deficient conditions. The mitochondrial membrane potential in *Cgatg32Δ* cells was significantly lower than that in wild-type cells under iron-depleted conditions. In a mouse model of disseminated infection, the *Cgatg32Δ* strain resulted in significantly decreased kidney and spleen fungal burdens compared with the wild-type strain. These results indicate that mitophagy in *C. glabrata* occurs in an iron-poor host tissue environment, and it may contribute to the longevity of cells, mitochondrial quality control, and pathogenesis.

### ARTICLE HISTORY

Received 3 March 2015  
Revised 18 April 2016  
Accepted 21 April 2016

### KEYWORDS

Atg32; autophagy; *Candida*; iron; mitochondria; mitophagy; pathogenicity; yeast

### Introduction

The number of immune-compromised individuals has increased because of HIV infection and population aging, and this clinical situation has provided opportunities for systemic infections by *Candida* spp. In candidiasis, a new emerging trend has been observed, where there has been a shift toward infections with non-*albicans* *Candida* species.<sup>1</sup> In particular, *C. glabrata* is now the second most important cause of fungal infections in humans.<sup>2</sup> However, little is known about the virulence factors that contribute to the pathogenesis of *C. glabrata*.

Mitochondria play a central role in cellular energy metabolism, where these organelles are essential for the generation of the ATP required for multiple cellular functions. They consume large amounts of molecular oxygen, and the mitochondrial respiratory chain is the major source of cytotoxic reactive oxygen species (ROS).<sup>3</sup> Thus, controlling the quality and quantity of mitochondria is essential in every eukaryotic organism.

Autophagy can be classified as bulk or selective. Mitophagy, the degradation of mitochondria via selective autophagic machinery, is thought to be involved in regulating the mass and function of mitochondria.<sup>4–8</sup> Mitophagy in yeast cells is efficiently

activated under nitrogen-starved conditions (following growth on a nonfermentable carbon source) or after long-term growth in nonfermentable medium conditions.<sup>7,8</sup> However, the physiological importance of mitophagy in this model organism and other yeast species remains largely unexplored. The mitochondrial protein Atg32, which is responsible for mitophagy, was identified in *S. cerevisiae*, and studies of Atg32 have helped to elucidate the detailed processes of mitophagy.<sup>7–10</sup>

Mitophagy is required for the longevity of *S. cerevisiae* during caloric restriction.<sup>11</sup> The mechanisms that confer longevity by mitophagy are considered to be related to the elimination of dysfunctional mitochondria.<sup>11</sup> The life span of yeast cells is determined by the cellular ROS and glutathione (GSH) levels, mitochondrial membrane potential (MMP), and the concentration of glucose in the medium,<sup>12–16</sup> but the details of the longevity-promoting mechanisms have not been fully elucidated.

In this study, we showed that the expression of *C. glabrata* (*Cg*) *ATG32* was upregulated and mitophagy was activated under iron-deficient conditions in *C. glabrata*. We compared the mitophagic activity, ROS production, MMP, and chronological life span (CLS)

**CONTACT** Koichi Tanabe  [ktanabe@agr.ryukoku.ac.jp](mailto:ktanabe@agr.ryukoku.ac.jp)  Department of Food Science and Human Nutrition, Faculty of Agriculture, Ryukoku University, 1-5 Yokotani, Seta Oe-cho, Otsu, Shiga 520-2194, Japan.

 Supplemental data for this article can be accessed on the [publisher's website](#).

© 2016 Minoru Nagi, Koichi Tanabe, Hironobu Nakayama, Keigo Ueno, Satoshi Yamagoe, Takashi Umeyama, Hideaki Ohno, and Yoshitsugu Miyazaki. Published with license by Taylor & Francis. This is an Open Access article distributed under the terms of the Creative Commons Attribution-Non-Commercial License (<http://creativecommons.org/licenses/by-nc/3.0/>), which permits unrestricted non-commercial use, distribution, and reproduction in any medium, provided the original work is properly cited. The moral rights of the named author(s) have been asserted.

of wild-type (WT) and *atg32Δ* mutant isogenic *C. glabrata* strains under iron-depleted conditions. Finally, we examined the importance of mitophagy in *C. glabrata* using mouse infection models.

## Results

### **Both the expression and phosphorylation of CgAtg32 are increased under iron-depleted conditions in *Candida glabrata***

During systemic infections, the amount of free iron supplied to *C. glabrata* cells is thought to be severely limited by iron-chelating proteins such as transferrin.<sup>17</sup> Thus, the iron-deficiency response in *C. glabrata* cells and other pathogenic microorganisms probably has important roles in their survival inside the host's body.<sup>18,19</sup> To investigate the response to iron deficiency in *C. glabrata*, we performed transcriptome analyses of cells grown under iron-replete (synthetic glucose medium; SD) and iron-depleted (SD medium without iron but with 100 μM ferrozine, which is a chelator of iron; SD-Fe) conditions. The expression level of a gene orthologous to *ATG32*, the essential gene for mitochondria-specific autophagy (mitophagy) in *Saccharomyces cerevisiae*, *CAGL0H06545g/CgATG32*, was upregulated in *C. glabrata* cells grown in SD-Fe medium (Table S1).

To verify the results of the transcriptome analysis, we investigated the expression of *CgATG32* under iron-depleted conditions by real-time RT-PCR. The expression level of *CgATG32* was 3-fold greater in cells grown in SD-Fe medium for 4 h compared with cells grown in SD medium (Fig. 1A). We further examined the expression level of *CgATG32* and *CgATG8* both of which are indispensable proteins for mitophagy during longer incubation periods (Fig. S2A, B). Time-course experiments showed that the amount of RNA of both *CgATG32* and *CgATG8* were decreased at 8-h incubation with SD-Fe, and increased again after a 24-h incubation.

It has been reported that the factors for mitophagy-induction in yeast are not only the expression level of *ATG32* but also the phosphorylation status of the corresponding protein.<sup>20–22</sup> Next, we performed western blot analysis to examine the phosphorylation status of CgAtg32 using a hemagglutinin (HA)-tagged *CgATG32* expressing strain (*atg32Δ* 3HA-*CgATG32*) (Fig. 1B). The apparent molecular mass of CgAtg32 on a SDS polyacrylamide gel was increased when the cells were grown either in SD or in SD-Fe medium on d 1. CgAtg32 was not detected after 2 d of incubation in SD-Fe medium whereas it was gradually decreased but still detectable on d 7 in SD medium. To determine whether these electrophoretic mobility shifts of CgAtg32 were due to phosphorylation, cellular protein extracts were treated with lambda protein phosphatase (λ PP) (Fig. 1C). The shifted CgAtg32 bands observed on day 0 and on d 1 with the test medium (SD or SD-Fe) disappeared following λ PP treatment, indicating that the shifted-band reflected the phosphorylated CgAtg32. Furthermore, the amount of both total and phosphorylated CgAtg32 was much higher in SD-Fe conditions than in iron-replete conditions. These results suggest that CgAtg32 is phosphorylated even in SD medium, and iron deficiency increases the amount of CgAtg32 and promotes further phosphorylation of this protein. Thus, we hypothesized that mitophagy was induced in *C. glabrata* under iron-depleted conditions and that mitochondrial degradation may play roles in the adaptation to iron deficiency.

### **Mitophagy is induced under iron-depleted conditions**

We examined mitophagy in *C. glabrata* cells under iron-depleted conditions. Cells expressing mitochondria-targeted mouse dihydrofolate reductase (Acc#; V00734.1)-GFP (mtDHFR-GFP) were grown in SD or SD-Fe medium, and proteolytic processing of mtDHFR-GFP was detected by western blotting with anti-GFP antibody. It is considered that mtDHFR-GFP is degraded to produce the GFP-moiety when mitophagy (involving the vacuolar degradation of mitochondria) is induced.<sup>8</sup> The processed GFP was detected in cells grown in SD-Fe medium for 36 and 48 h, but not in SD medium (Fig. 1D). We also performed a mtDHFR-GFP processing assay with mutant cells that lacked the orthologous genes of *S. cerevisiae* *ATG32* (*Cgatg32Δ*), *ATG1* (*Cgatg1Δ*), and *ATG11* (*Cgatg11Δ*). In *S. cerevisiae*, *ATG1* is indispensable for bulk and selective autophagy, whereas Atg11 is required primarily for the latter.<sup>10,23,24</sup> The release of GFP from mtDHFR-GFP in SD-Fe medium at 48 h was eliminated completely in every *atg* null mutant (Fig. 1E). Furthermore, we validated the GFP-localization to the vacuole in WT cells but not in *Cgatg32Δ* cells grown with SD-Fe by fluorescence microscopy observation (Fig. S3A). These results suggest that mitophagy is induced in *C. glabrata* under iron-depleted conditions, and that *CgATG32*, *CgATG1*, and *CgATG11* are essential genes for mitophagy in *C. glabrata* as well as in *S. cerevisiae*.

### **Mitophagy is induced in long-term culture, but is not immediately induced by nitrogen starvation**

In *S. cerevisiae*, mitophagy is immediately induced (2–4 h) when cells are cultured under nitrogen-starved conditions after preculturing in nonfermentable medium.<sup>7</sup> In addition, it has also been reported that nonfermenting long-term culture (> 2 d) induce mitophagy.<sup>8</sup> We performed the mtDHFR-GFP processing assay with *C. glabrata* cells grown in long-term culture or in nitrogen-starvation medium. The released GFP moiety was detected using cells grown in nonfermentable medium with glycerol (YPG) for 2–5 d (Fig. 2A) as well as in *S. cerevisiae*. The processing of mtDHFR-GFP was not detected in *Cgatg32Δ* mutant cells grown in YPG medium (Fig. 2A), indicating that *CgATG32* is also responsible for mitophagy in nonfermented long-term culture. Conversely, the released GFP was not detected using cells grown in nitrogen-starvation medium (SD-N) for 0–6 h (Fig. 2B). For longer incubation (1–3 d) in SD-N medium, the free GFP was finally detected in *C. glabrata* (Fig. S4B; longer exposure image of blot). The mtDHFR processing assay also showed that the amount of processed GFP moiety under iron-depleted conditions was substantially higher than that observed in nonfermentative or nitrogen-starved long-term culture (Fig. S4A, C). These results suggest that iron depletion rather than long-term culture or nitrogen-starved conditions strongly induces mitophagy in *C. glabrata*. In contrast, iron depletion did not promote mtDHFR-GFP processing in *S. cerevisiae* (Fig. S4D). These data suggest that the extracellular signals that potentially induce mitophagy are partly conserved yet different between *S. cerevisiae* and *C. glabrata*.

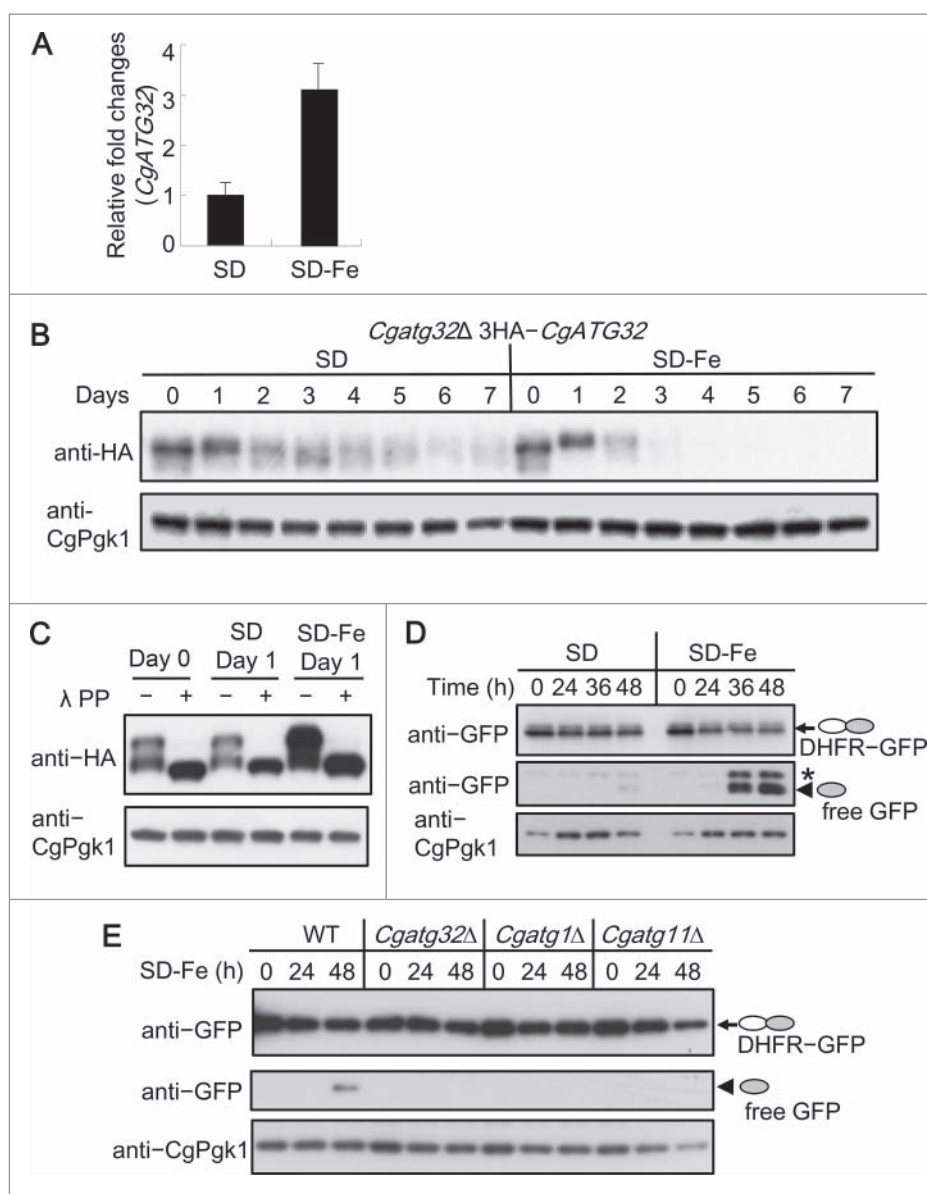


**Figure 1.** Mitophagy induced in *C. glabrata* under iron-depleted conditions. (A) cDNA was prepared using total RNA from  $6 \times 10^6$  cells incubated under iron-replete (SD medium) or iron-depleted (SD-Fe medium) conditions at 30°C for 4 h. Quantitative RT-PCR analysis was performed. The expression of *CgATG32* in cells incubated in SD-Fe medium is shown as the relative fold change compared with cells incubated in SD medium. The values represent the mean and standard deviation of triplicate measurements based on a representative experiment. (B) The phosphorylation status of CgAtg32 was assessed using an HA-tagged *CgATG32*-expressing strain (*Cgatg32Δ* 3HA-*CgATG32*) by western blotting. *Cgatg32Δ* 3HA-*CgATG32* cells were grown in SD or SD-Fe medium, and collected at the indicated time points, and then subjected to western blot analysis with anti-HA and anti-CgPgk1 (loading control) antibodies. (C) *Cgatg32Δ* 3HA-*CgATG32* cells were grown in SD or SD-Fe medium for 1 d. Cell lysates were treated with or without  $\lambda$  PPase at 30°C for 1 h. The phosphatase-treated samples were subjected to western blotting with anti-HA or anti-CgPgk1 (loading control) antibodies. (D) KUE200 (wild-type) cells expressing mtDHFR-GFP were grown in SD or SD-Fe medium, and collected at the indicated time points, and then subjected to western blot analysis with anti-GFP antibody. mtDHFR-GFP and the processed GFP moiety are indicated by the arrow and arrowhead, respectively. The generation of processed GFP indicates the vacuolar degradation of mtDHFR-GFP. CgPgk1 was monitored as a sample loading control. Nonspecific bands are designated by an asterisk. (E) KUE200 (wild-type), *Cgatg32Δ*, *Cgatg1Δ*, and *Cgatg11Δ* strains expressing mtDHFR-GFP were cultured in SD-Fe medium, collected at the indicated time points, and then subjected to western blot analysis with anti-GFP and anti-CgPgk1 (loading control) antibodies.

### Inhibition of mitochondrial functions does not induce mitophagy

The respiratory activity of *C. glabrata* cells grown in SD-Fe medium is thought to be decreased because some key respiratory enzymes require iron for their function.<sup>25,26</sup> Thus, we hypothesized that mitochondrial degradation in *C. glabrata* is also induced by respiratory inhibition. However, no mtDHFR-GFP processing was observed in anaerobically cultured cells (Fig. 3). Subsequently, the mtDHFR-GFP processing assay was performed using cells grown under conditions where mitochondrial function was attenuated.

The addition of carbonyl cyanide *m*-chlorophenyl hydrazone, an uncoupler of oxidative phosphorylation, or antimycin A, a mitochondrial electron transport inhibitor, did not induce mitophagy (Fig. 3). These results indicate that mitochondrial dysfunction alone could not initiate mitophagy in *C. glabrata*.

### *CgAtg32* is required for longevity under iron-depleted conditions

It has been reported that mitophagy confers longevity on *S. cerevisiae* under nitrogen-starved conditions.<sup>11</sup> Thus, we

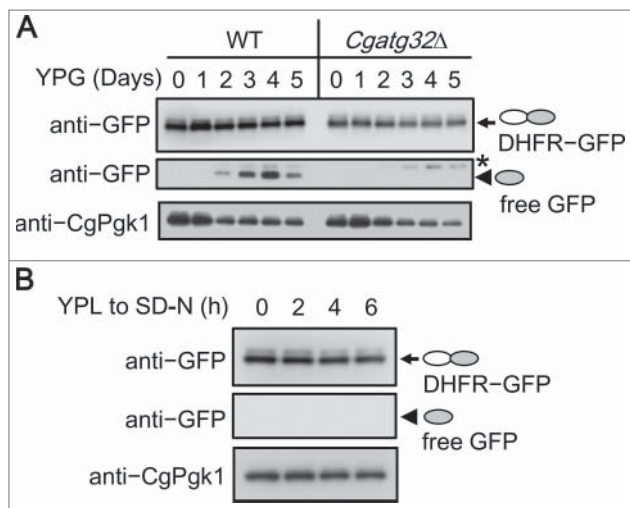


**Figure 2.** Nonfermented long-term culturing but not short-period nitrogen starvation induces mitophagy in *C. glabrata*. (A) KUE200 (WT) and *Cgatg32Δ* strains expressing mtDHFGR-GFP were cultured in glycerol medium (YPG), collected at the indicated time points, and then subjected to western blot analysis with anti-GFP and anti-CgPgk1 (loading control) antibodies. Nonspecific bands are designated by an asterisk. (B) mtDHFGR-GFP-expressing KUE200 cells were cultured in lactate medium (YPL) to the mid-log growth phase, then shifted to nitrogen-depleted (SD-N) medium for 0, 2, 4, and 6 h. The processing of mtDHFGR-GFP was monitored by western blotting with anti-GFP antibody, and anti-CgPgk1 antibody for loading control.

compared the CLS of the WT, *Cgatg32Δ* and *Cgatg32Δ CgATG32* transformed *C. glabrata* strain in iron-depleted medium. The *C. glabrata* strains were cultured in the SD or SD-Fe medium, and the number of colony-forming units (CFUs) and the OD<sub>600</sub> of aliquots of each culture were measured at specific times. WT and *Cgatg32Δ CgATG32* cultures retained 10% viable cells until d 12 under any growth conditions, whereas the *Cgatg32Δ* mutant cells lost viability in SD-Fe medium at d 5 (Fig. 4A). Thus, mitophagy is thought to be an essential longevity assurance process in chronologically aging *C. glabrata* grown under iron-deficient conditions.

### ROS accumulation in *C. glabrata* cells under iron-deficient conditions

The amount of cellular ROS increases in the *atg32Δ* mutant of *S. cerevisiae* compared with WT cells under nitrogen starvation conditions.<sup>4</sup> Thus, we hypothesized that mitophagy-deficient *Cgatg32Δ C. glabrata* cells would accumulate ROS under iron-

depleted conditions and that the excess amount of ROS would reduce the CLS because the accumulated ROS should cause DNA damage and oxidative stress, thereby inhibiting cellular proliferation in eukaryotes.

We quantified the amount of cellular ROS by flow cytometry analyses of cells stained with dihydroethidium (DHE), which reacts mainly with superoxide (Figs. 5A, B, S5A–D). In SD medium, both the cellular ROS levels and the ratio of ROS-positive cells did not differ significantly in the WT, *Cgatg32Δ* and *Cgatg32Δ CgATG32* cells. Unexpectedly, both the cellular ROS levels and the ratio of ROS-positive cells in the WT and *Cgatg32Δ CgATG32* cells were greater than those in the *Cgatg32Δ* mutant under iron-deficient conditions. The amount of oxidized proteins, which reflects the intracellular ROS level, also indicated that the ROS level was higher in the WT than *Cgatg32Δ* cells (Fig. 5C). These results suggest that the decreased cellular ROS levels under iron-deficient conditions are related to the lack of mitophagy in *Cgatg32Δ* cells.

### Mitophagy is involved in MMP maintenance under iron-deficient conditions

The major component of the mitochondrial electrochemical potential gradient of protons is MMP, which is a parameter used to assess mitochondrial function and cellular longevity. The MMP was quantified by staining cells with the fluorescent membrane potential-dependent dye 3,3'-dihexyloxacarbocyanine iodide (DiOC<sub>6</sub>[3]) and the fluorescence was evaluated using a flow cytometer. In SD medium, both the mean cellular MMP levels and the ratio of MMP-positive cells did not differ significantly between WT, *Cgatg32Δ* and *Cgatg32Δ CgATG32* cells (Figs. 6A, B, S6A, B). Iron-depletion decreased the 2 MMP parameters in the cells of all 3 strains, but the parameters for the WT and *Cgatg32Δ CgATG32* cells were higher than those for the *Cgatg32Δ* mutant under iron-deficient conditions (Figs. 6A, B, S6C, D). These results suggest that mitophagy is required for MMP maintenance under iron-deficient conditions.

### Disruption of CgATG32 reduces the virulence of *C. glabrata* in a mouse model of disseminated infection

The possible role of mitophagy during disseminated infection was tested in a mouse infection model. Mice were inoculated intravenously with the WT strain, *Cgatg32Δ* mutant, or

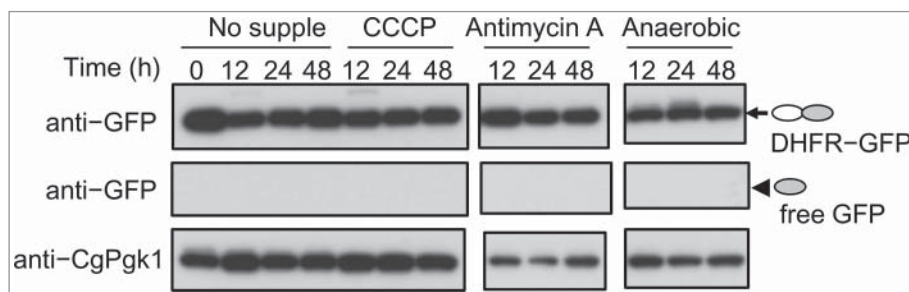


**Figure 3.** Inhibition of respiration or mitochondrial functions do not induce mitophagy in *C. glabrata*. mtDHFGR-GFP-expressing KUE200 (wild-type) cells were grown in SD medium with or without the indicated supplements (4 μg/mL carbonyl cyanide m-chlorophenyl hydrazone [CCCP]; 8 μg/mL antimycin A), or under anaerobic growth condition, collected at the indicated time points, and then subjected to western blot analysis with anti-GFP and anti-CgPgk1 (loading control) antibodies.

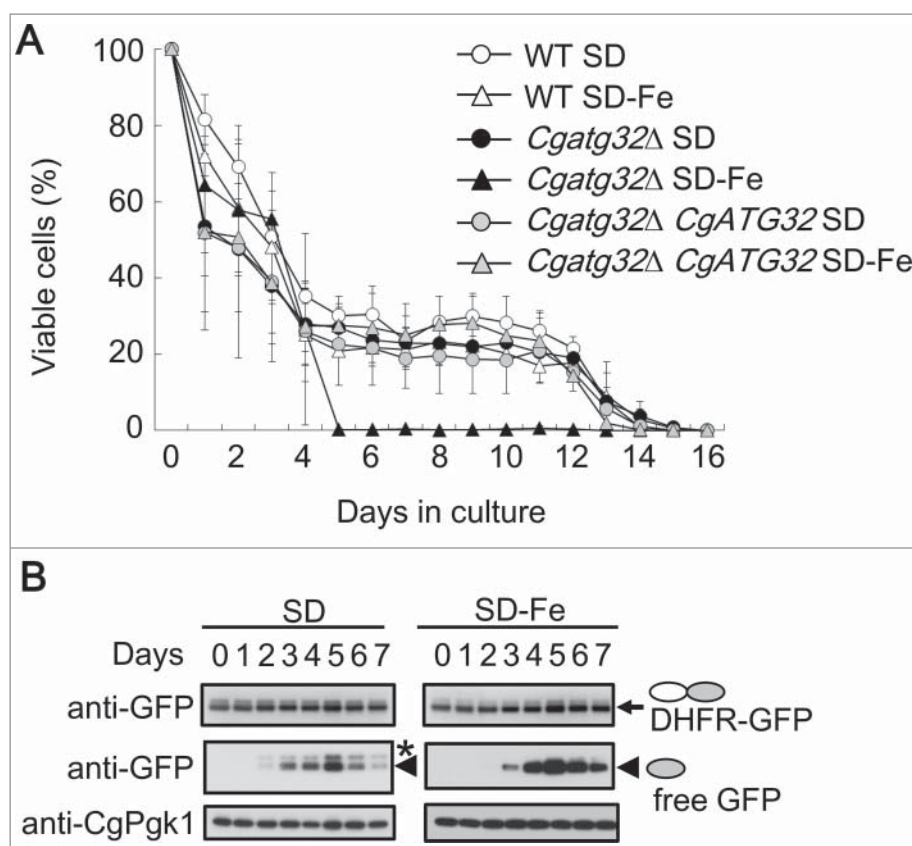


**Figure 4.** Mitophagy is required for the longevity of *C. glabrata* under iron-deficient conditions. (A) Chronological life-span assay (colony-forming units per whole cell number) of KUE200 (wild-type), *Cgatg32*Δ, and *Cgatg32*Δ *CgATG32* cultured in SD or SD-Fe medium. The mean ± SEM values are representative of 3 independent experiments. (B) mtDHFGR-GFP-expressing wild-type cells were grown in SD or SD-Fe medium, collected at the indicated time points, and then subjected to western blot analysis with anti-GFP and anti-CgPgk1 (loading control) antibodies. Nonspecific bands are designated by an asterisk.

revertant cells (the *Cgatg32*Δ mutant transformed with *CgATG32*). In mice infected with the *Cgatg32*Δ strain, the number of cells recovered from kidneys was about 6 times lower than that from mice infected with either the WT or the revertant strain (Fig. 7A). The cell numbers recovered from the spleen when infected with the 3 strains were similar to the results obtained with the kidneys (Fig. 7B).

The expression of *CgATG32* was also examined in cells recovered from the kidneys of immune-compromised mice infected with the WT strain. The *CgATG32* expression level was about 6 times greater in cells recovered from mouse kidneys compared with that in cells grown in vitro without supplements (Fig. 7C). These results suggest that mitophagy in *C. glabrata* cells is an indispensable event for survival inside host organs.

## Discussion

During systemic infections, the amount of free iron supplied for the growth of *C. glabrata* cells is severely suppressed by iron-chelating proteins such as transferrin.<sup>17</sup> It is considered that the iron deficiency response in *C. glabrata* cells is indispensable for their survival inside the host's body. Our transcriptome analysis showed that the expression level of the gene homologous to *S. cerevisiae* *ATG32*, which encodes a mitochondrial outer membrane protein required for the initiation of mitophagy, was upregulated under iron-depleted conditions in *C. glabrata* (Fig. 1A, Table S1). This raised the possibility that mitophagy

contributes to the stress responses in *C. glabrata* cells in an iron-deficient environment.

The mtDHFGR-GFP processing assay and microscopy observation of the *C. glabrata* strain expressing mtDHFGR-GFP supported the existence of mitophagy (selective vacuolar mitochondria degradation) in *C. glabrata* grown under iron-depleted conditions (in SD-Fe). To obtain other evidence for mitophagy, a mitochondrial inner membrane protein, CgCox2, and an outer membrane protein, CgPor1, were quantified by western blotting to examine the amount of mitochondria (Fig. S3B). The amount of CgPor1 seemed to be constant even when mitophagy was activated (day 2–7) whereas that of CgCox2 was gradually decreased until d 7. The decrease of CgCox2 was also observed in cells grown under iron-replete conditions (SD medium) at a slower rate than in cells grown in SD-Fe. The slow decrease of CgCox2 in SD medium may reflect the low mitophagic activity (highly activated mitophagy resulted in a fast decrease of CgCox2 in SD-Fe) (Fig. 4B). The uneven change in the amount of inner and outer mitochondrial membrane protein indicates a change in quality (or structure) but not in quantity of mitochondria. These observations demonstrated an interesting aspect of mitophagy, and further characterization of mitochondria should be performed.

We added 100 μM ferrozine to the iron-depleted medium to mimic the free ferric ion concentration inside the host body. The concentration of free ferric ion inside human serum was thought to be extremely low (~10<sup>-24</sup> M).<sup>27</sup> A strong iron chelator was

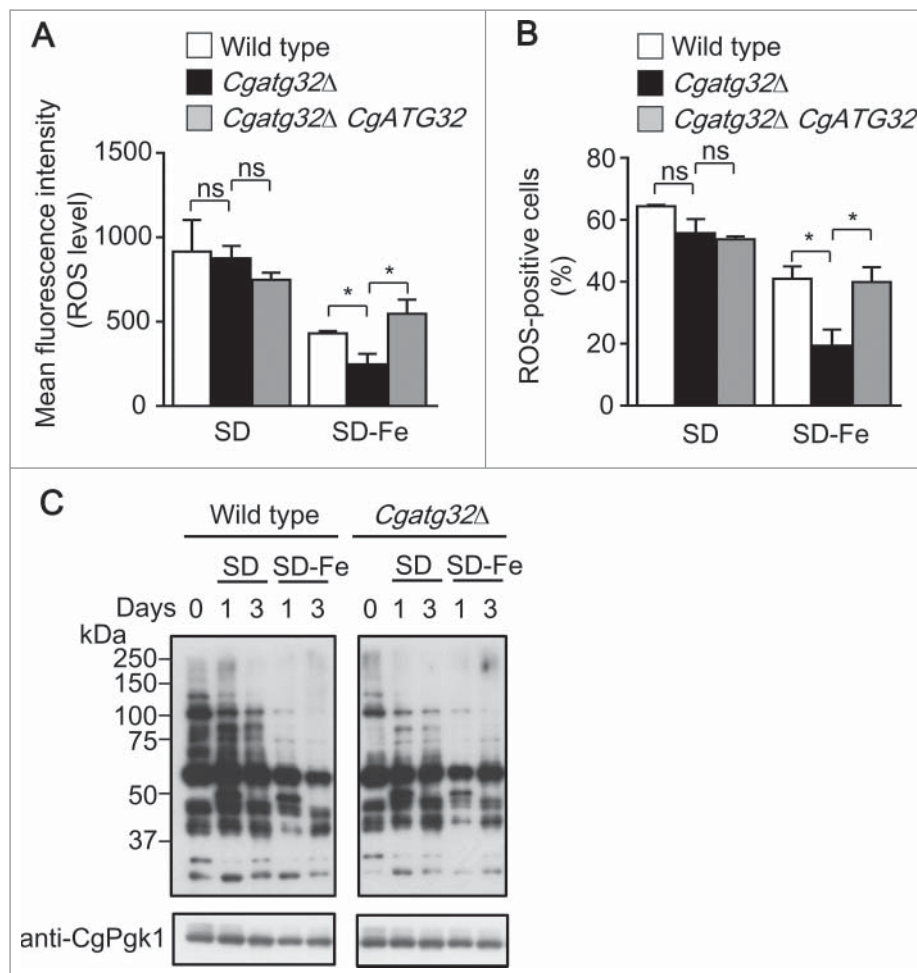


**Figure 5.** Loss of mitophagy results in decreased intracellular ROS. Wild-type, *Cgatg32Δ*, and *Cgatg32Δ CgATG32* cells were cultivated for 3 d under the indicated growth conditions. The mean ROS levels (A) and the ratio of ROS-positive cells (B) were determined by flow cytometric analyses of cells treated with dihydroethidium. The mean  $\pm$  SEM values are representative of 3 independent experiments. Asterisks indicate statistically significant differences (\*,  $P < 0.05$ ). ns indicates no significant difference ( $P > 0.05$ ). (C) Wild-type and *Cgatg32Δ* cells were cultured in SD, SD-Fe, or SD-Fe. After the indicated incubation period, oxidized proteins were detected by an OxyBlot assay.

required for almost complete depletion of free ferric ion. However, it seemed to be difficult to obtain perfectly reproducible results from cells grown in SD-Fe probably due to the huge amount of iron supplied from the nutrient-rich preculture prior to shifting to SD-Fe. For example, the GFP moiety in the mtDHFR-GFP processing assay was detected on d 2 after being shifted to SD-Fe in most experiments, whereas it was detected on d 3 in Figure 4B. The amount of GFP-moiety detected on d 2 might be easy to cause to fluctuate by subtle differences in growth conditions, as they were much lower than those on d 4–5. We assume the results obtained from cells grown in SD-Fe were virtually reproducible; however, other iron-depleted conditions should be tested for further examination.

Because the genes related to autophagy in *S. cerevisiae* are highly conserved in *C. glabrata*, we expected that autophagy and mitophagy would involve similar molecular mechanisms in both yeast species. Disruption of the genes homologous to *S. cerevisiae* *ATG32*, *ATG1*, and *ATG11* (required for mitophagy, all types of autophagy, and selective autophagy, respectively) blocked mitochondrial degradation completely (Fig. 1E). The phosphorylation of CgAtg32 before mitophagy was also detected in iron-depleted *C. glabrata* cells (Fig. 1C) as observed in *S. cerevisiae* under nitrogen-starved conditions. These

observations further support the existence of conserved autophagic/mitophagic machinery between 2 genetically related yeast species. The expression of genes indispensable for mitophagy, *CgATG8* and *CgATG32*, was elevated at 4 h after the shift to iron-depleted conditions, dropped down at 8 h, and increased again during 24–48 h of incubation (Fig. S2A, B). The re-induction of *ATG* genes before 48 h may support the initiation of mitophagy on d 2; however, the role of the initially enhanced expression of the genes (at 4 h) is unclear. The sudden decrease in mRNA of the *ATG* genes at 8 h is curious. The reduction of mRNA was only partly suppressed in the autophagy-deficient *atg1Δ* mutant (Fig. S2C, D). These results suggest that some autophagic degradation may participate in the reduction of mRNA at 8 h under iron-depleted conditions; however, the rapidly increased cell number during the growing phase or the spontaneous mRNA degradation may also contribute to the reduced cellular mRNA of the *ATG* genes.

In *S. cerevisiae*, mitophagy was induced: (i) in nonfermented long-term culture, or (ii) short-period exposure to nitrogen-starved conditions after preculturing in nonfermentable medium.<sup>7,8</sup> Figures 2 and S4 revealed that nitrogen-starvation may be the common mitophagy-inducing condition for both *S. cerevisiae* and *C. glabrata*, whereas iron-depletion strongly

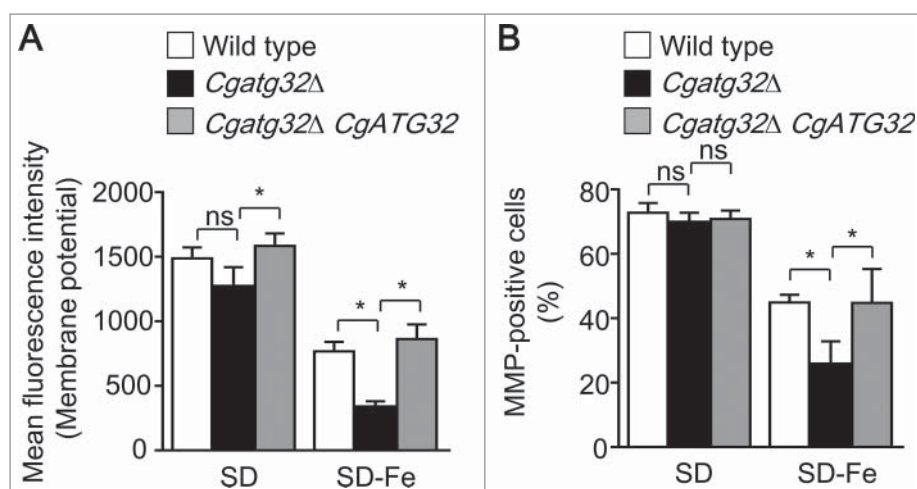


**Figure 6.** Mitophagy is required for maintenance of mitochondrial membrane potential. Wild-type, *Cgatg32Δ*, and *Cgatg32Δ CgATG32* cells were cultivated for 3 d under the indicated growth conditions. The mean MMP levels (A) and the ratio of MMP-positive cells (B) were determined by flow cytometric analyses of cells treated with DiOC<sub>6</sub>(3). The mean values  $\pm$  SEM are representative of 3 independent experiments. Asterisks indicate statistically significant differences (\*,  $P < 0.05$ ). ns indicates no significant difference ( $P > 0.05$ ).

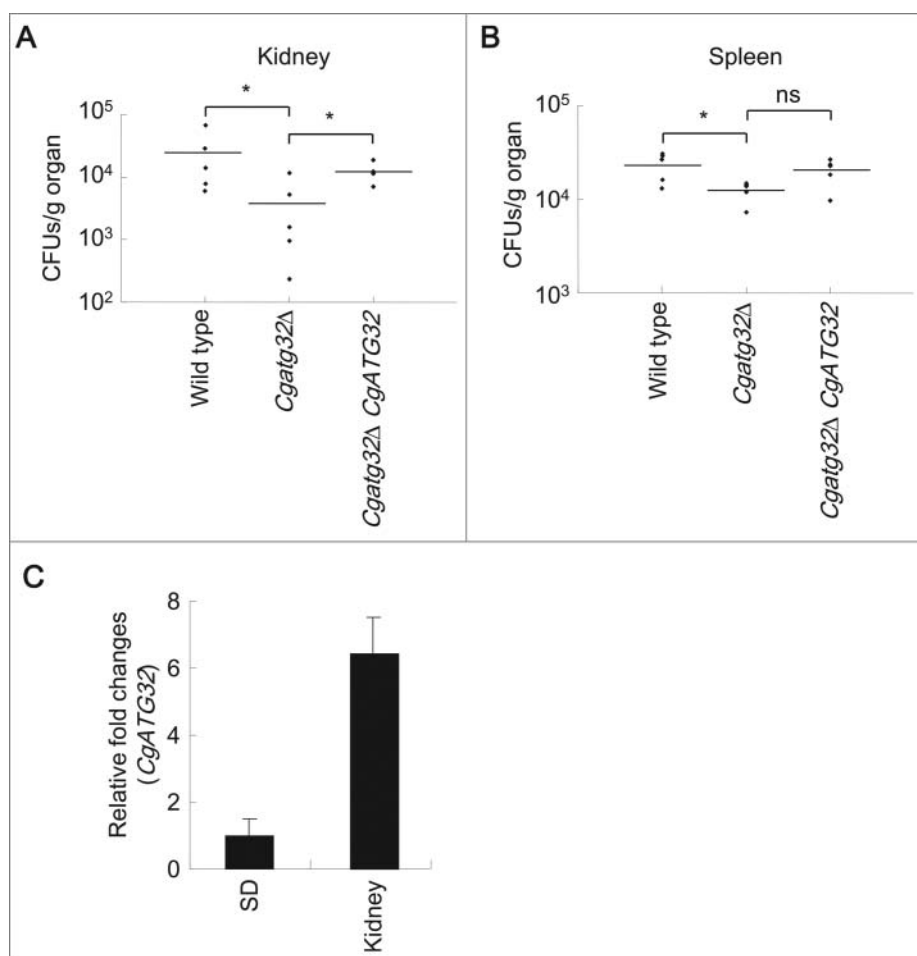


**Figure 7.** ATG32 is required to maintain the fungal burden in mouse tissues. (A, B) Fungal tissue burdens in the kidney (A) and spleen (B) from groups of 5 BALB/c mice infected via the tail vein with  $1 \times 10^7$  viable cells of *C. glabrata* strains. The results are expressed as CFU/g of tissue and they represent values recorded separately in each of the 5 mice. Geometric means are indicated by horizontal bars. Statistical comparisons are summarized above each panel. Asterisks indicate statistically significant differences (\*,  $P < 0.05$ ). NS indicates no significant difference ( $P > 0.05$ ). (C) Immuno-suppressed CD-1 mice were inoculated with the *C. glabrata* wild-type strain CBS138. Mice were rendered neutropenic via intraperitoneal administration of cyclophosphamide (200 mg/kg of body weight per day) and cortisone acetate (125 mg/kg of body weight per day) 3 d before challenge and on the day of infection. Mice were injected with  $1 \times 10^6$  viable cells. After 7 d, the mice were sacrificed and their kidneys were excised. Yeast present in excised kidneys were collected by pipette and transferred to a 1.5-mL collecting tube on ice. The collected cells were used in the expression analyses. The expression of *CgATG32* is represented as the relative fold change compared with wild-type cells incubated under aerobic conditions at 30°C for 4 h. The values represent the mean and standard deviation based on triplicate measurements from a representative experiment.

induced mitophagy in *C. glabrata* alone. These results suggest that the regulatory mechanisms of mitophagy are partly conserved but different between the 2 yeast species. The difference in the mitophagy-inducing conditions for these 2 yeasts may be explained by variations in their usual growth environments and evolutionary gene rearrangements. Comparative genome analyses of *S. cerevisiae* and *C. glabrata* indicate that *C. glabrata* has lost genes involved in galactose, phosphate, nitrogen, and sulfur metabolism via genome evolution from the common ancestor of *S. cerevisiae*. As a result of these gene losses, *C. glabrata* exhibits auxotrophy for some nutrients such as nicotinic acid, pyridoxine, and thiamine.<sup>28,29</sup> *C. glabrata* is thought to have undergone this reductive evolution to suit the host environment, like other pathogenic microorganisms.<sup>30</sup> It is possible that *C. glabrata* has lost the genes responsible for mitophagy induction in response to short-period nitrogen starvation and it may have gained another mitophagic regulation system to survive inside the host's body. *C. glabrata* is assumed to regulate mitochondrial function by mitophagy to survive in an iron-deficient environment, such as a host's body. In iron-deficient conditions, both heme biosynthesis and respiratory activity could be inhibited.<sup>25,26</sup> Therefore, in *C. glabrata*, it is expected that dysfunctional mitochondria are degraded by mitophagy to maintain mitochondrial homeostasis. Along these lines, PINK1-PARK2-independent mitophagy was reported in human osteosarcoma or neuroblastoma cells under iron-depleted conditions.<sup>31</sup> Thus, iron depletion may be the common initiation signal for mitophagy among some eukaryotes.

Mitophagy is also responsible for the prolonged life span of *S. cerevisiae* during caloric restriction.<sup>11</sup> In a mitophagy-deficient mutant strain (*atg32Δ*) of *S. cerevisiae* which exhibits shortened CLS, the ROS level is increased whereas MMP is decreased compared with those in the WT.<sup>4</sup> In terms of the relationship between life span and ROS, 2 opposite effects of ROS have been proposed in *S. cerevisiae*.<sup>12,16,32–34</sup> It has been reported that ROS accumulation after the deletion of *FLX1*, which catalyzes the movement of the redox cofactor FAD across the mitochondrial membrane, shortens the life span.<sup>35</sup> By contrast, Mesquita et al. reported that increased intracellular ROS levels due to the inactivation of Cta1 or Ctt1, the 2 main ROS-scavenging enzymes, extend the CLS.<sup>12</sup> They also demonstrated that the decreased intracellular ROS caused by the overexpression of *CTA1* results in a shortened CLS.<sup>12</sup> The discrepancy above could be partly illustrated by the “mitochondrial ROS signaling;” ROS are generally thought to shorten life span by bringing about oxidative damage on DNA or essential enzymes required for cell division; however, the elevated ROS level during the growing phase enhances oxidative stress responses, increases the intracellular enzymes that detoxicate ROS during stationary phase, and result in elongated CLS.<sup>36</sup> In regard to MMP, it was reported that a reduction in the MMP in old cells or in the presence of dinitrophenol, a mitochondrial uncoupler, leads to a decreased life span.<sup>37–39</sup> Thus, it is considered that MMP is maintained to support the intracellular ATP levels, thereby retaining the longevity of *S. cerevisiae*.

In the present study, we found that the disruption of *CgATG32* reduced the life span of *C. glabrata* cells under iron-

depleted conditions as in the case of *S. cerevisiae* under caloric-restricted condition (Fig. 4A). The MMP in *Cgatg32Δ C. glabrata* was lower than that in WT cells (Figs. 6A, B, S6A–D) as expected from the result of *S. cerevisiae*, whereas the ROS in the mutant was lower than that in WT (Figs. 5A, B, S5A–D). In the case of *C. glabrata* grown under iron-depleted conditions, it is possible that the decreased ROS in *Cgatg32Δ* cells during the growing phase, failed to evoke mitochondrial ROS signaling, and resulted in the decreased CLS. These findings also indicate that mitophagy during the growing phase may be necessary for keeping active respiration in mitochondria and for induction of mitochondrial ROS signaling before entering stationary phase. However, these hypotheses need to be examined by further study with *C. glabrata* cells under other growing conditions or by other ROS-detection reagents.

We also found that supplementation of SD-Fe medium with N-acetyl-L-cysteine (NAC), a potential ROS scavenger, restored the decreased CLS of *Cgatg32Δ* cells to the level of WT cells (Fig. S7A). This result prompted us to hypothesize that the restored CLS of *Cgatg32Δ* by NAC was due to scavenging of ROS; however, the ROS level of *Cgatg32Δ* was less than that of WT cells under iron-depleted conditions as mentioned above (Fig. 5A, B). Moreover, NAC-treatment did not decrease ROS levels or protein oxidation of either WT or *Cgatg32Δ* cells (Fig. S8A–C). Decreased MMP in *Cgatg32Δ* cells was also unaffected by NAC-treatment (Fig. S9). In terms of ROS scavenging, the effect of NAC on improved CLS of *Cgatg32Δ* is completely unexplained; however, it is possible that NAC scavenged a kind of minor ROS, which are not detected in this study but are nonetheless harmful to replication.

NAC-treatment also suppressed mitophagy in *C. glabrata* grown under iron-depleted conditions (Fig. S7B, C). NAC stimulates GSH synthesis after its conversion into cysteine, and is a mitophagy inhibitor in *S. cerevisiae*.<sup>40</sup> Supplementation with N-acetyl-D-cysteine, an optical isomer of NAC with similar ROS scavenging properties to NAC but that does not promote GSH synthesis, does not inhibit mitophagy.<sup>40,41</sup> Direct supplementation of GSH monoethylester in yeast cells successfully inhibits mitophagy.<sup>40</sup> These previous results with *S. cerevisiae* suggest that the promotion of GSH synthesis may inhibit mitophagy during NAC treatment without the reduction of cellular ROS level. It has also been reported that CLS is increased by pharmacological inhibition of the synthesis of glutathione using L-buthionine-sulfoximine.<sup>12</sup> Thus, there may be a relationship between longevity and regulation of the GSH content.

In mice infection models with *C. glabrata*, we found that the deletion of *CgATG32* resulted in decreased kidney and spleen fungal burdens (Fig. 7). Since the expression of *CgATG32* was increased in the host's kidney, mitophagy is expected to be induced during infection and it is involved in the survival of the host tissue when depleted of free iron ions. The functions of mitochondria are thought to be inhibited by low oxygen and iron concentrations inside the host's body, so mitochondria may be less necessary during infections than in aerobic growth conditions. Another possible physiological role of mitophagy in *C. glabrata* cells may be the degradation of unnecessary mitochondria to replenish the amino acid pool.

Most pathogens that can potentially cause bloodstream infections are thought to have developed highly efficient iron acquisition systems, including siderophores, low molecular weight organic chelators with a high affinity for Fe<sup>3+</sup>, to survive inside the host's body. *C. glabrata* does not appear to possess the ability to synthesize siderophores or to efficiently utilize heme as an iron source.<sup>19</sup> This indicates that the iron deficiency response of this fungus differs from that of other pathogenic microorganisms.

Mitophagy is thought to be involved in controlling the quantity and quality of mitochondria in *S. cerevisiae*,<sup>4</sup> however the physiological importance of mitophagy was still unclear. Our results in this study support the idea that mitophagy is necessary for intact pathogenicity of *C. glabrata* cells probably through maintaining mitochondrial functions during infection. This study is for the first time proposing a physiological significance of mitophagy in a eukaryotic unicellular microorganism. Our results may also contribute to understanding the general role of mitophagy in higher eukaryotic organisms.

## Materials and methods

### Ethics

All our animal experiments were in compliance with the guidelines and policies of the Principles of Morality for Animal Experiments of the National Institute of Infectious Disease, Japan (approval number 114118-2).

### Strains and growth media

*Escherichia coli* DH5 $\alpha$  (F<sup>-</sup>,  $\phi$ 80, lacZ $\Delta$ M15,  $\Delta$  (lacZYA-argF) U169, hsdR17(rk<sup>-</sup> mk<sup>+</sup>), recA1, endA1, deoR, thi-1, supE44, gyrA96, relA1  $\lambda$ -) was used for plasmid propagation. Bacterial strains were grown in LB with 50  $\mu$ g/mL ampicillin. The growth media for yeast were as follows: YPD (1% yeast extract, 2% peptone, 2% glucose), YPL (1% yeast extract, 2% peptone, 2% lactate, pH 5.5), YPG (1% yeast extract, 2% peptone, 3% glycerol), SD (0.67% yeast nitrogen base, 2% glucose, amino

acids, vitamins), SD-Fe (SD without iron but with 100  $\mu$ M ferrozine [Sigma-Aldrich, 160601], which is a chelator of iron), SD-N (0.17% yeast nitrogen base without amino acids, 2% glucose; for nitrogen-starvation). Yeast strains and plasmids used in this study are listed in Table 1.<sup>8,42,43</sup>

### Construction of *CgATG* gene-disrupted *C. glabrata* strains

The DNA fragment used to replace the *CgATG32*, *CgATG1*, or *CgATG11* ORF with *CgHIS3* was amplified from the plasmid pHIS916<sup>42</sup> using the primer sets ATG32DF and ATG32DR, ATG1DF and ATG1DR, or ATG11DF and ATG11DR, respectively. Each amplified fragment (approximately 1 kb) was used to transform KUE200. Disruption of the *CgATG* genes was confirmed by PCR using primers pTET12F and ATG32CHR for *CgATG32*, pTET12F and ATG1CHR for *CgATG1*, and pTET12F and ATG11CHR for *CgATG11*, respectively. The sequences of all the primers are listed in Table S2. Integration of DNA fragments into the *CgATG32* gene locus was also confirmed by Southern blot analysis (Fig. S1).

### Introduction of *mtDHFR-GFP* into KUE200 and *ATG* gene mutants

A transformation cassette containing the mitochondria-targeted dihydrofolate reductase-GFP flanked by sequences upstream and downstream of *URA3* was amplified by PCR from p416GPD-*mtDHFR-GFP*<sup>8</sup> using the primers *mtDHFR* CST F and *mtDHFR* CST R, and used to transform KUE200 and *CgATG* gene-disrupted strains. Ura<sup>-</sup> transformants were selected on synthetic medium (0.67% [w/v] yeast nitrogen base [Difco, Becton, Dickinson and Company, 291940], 2% [w/v] glucose and 2% [w/v] agar, pH 7.0) containing 0.2% 5-fluoroorotic acid hydrate (Sigma-Aldrich, F5013). Accurate insertion of the amplified fragment into the correct chromosomal locus was confirmed by PCR using the primers *HIS3* up -100 to -80 and *GPD* pro 200-180. The sequences of all the primers are listed in Table S2.

**Table 1.** Strains and plasmids used in this study.

Strain	Genotype or feature <sup>a</sup>	Reference
CBS138	ATCC type culture	
KUE200	<i>trp1</i> $\Delta$ <i>his3</i> $\Delta$ :: <i>ScURA3</i> <i>ura3</i> $\Delta$ <i>FRT-YKU80</i>	42
<i>Cgatg32</i> $\Delta$	<i>trp1</i> $\Delta$ <i>his3</i> $\Delta$ :: <i>ScURA3</i> <i>ura3</i> $\Delta$ <i>FRT-YKU80</i> <i>atg32</i> $\Delta$ :: <i>HIS3</i>	This study
<i>Cgatg1</i> $\Delta$	<i>trp1</i> $\Delta$ <i>his3</i> $\Delta$ :: <i>ScURA3</i> <i>ura3</i> $\Delta$ <i>FRT-YKU80</i> <i>atg1</i> $\Delta$ :: <i>HIS3</i>	This study
<i>Cgatg11</i> $\Delta$	<i>trp1</i> $\Delta$ <i>his3</i> $\Delta$ :: <i>ScURA3</i> <i>ura3</i> $\Delta$ <i>FRT-YKU80</i> <i>atg11</i> $\Delta$ :: <i>HIS3</i>	This study
<i>Cgatg32</i> $\Delta$ <i>CgATG32</i>	<i>trp1</i> $\Delta$ <i>his3</i> $\Delta$ :: <i>ScURA3</i> <i>ura3</i> $\Delta$ <i>FRT-YKU80</i> <i>atg32</i> $\Delta$ :: <i>HIS3-ATG32-TRP1</i>	This study
<i>Cgatg32</i> $\Delta$ 3HA- <i>CgATG32</i>	<i>trp1</i> $\Delta$ <i>his3</i> $\Delta$ :: <i>ScURA3</i> <i>ura3</i> $\Delta$ <i>FRT-YKU80</i> <i>atg32</i> $\Delta$ :: <i>HIS3-3HA-ATG32-TRP1</i>	This study
KUE200- <i>mtDHFR-GFP</i>	<i>trp1</i> $\Delta$ <i>his3</i> $\Delta$ :: <i>GPD</i> <sup>P</sup> - <i>mito-mouse DHFR-GFP</i> <i>ura3</i> $\Delta$ <i>FRT-YKU80</i>	This study
<i>Cgatg32</i> $\Delta$ - <i>mtDHFR-GFP</i>	<i>trp1</i> $\Delta$ <i>his3</i> $\Delta$ :: <i>GPD</i> <sup>P</sup> - <i>mito-mouse DHFR-GFP</i> <i>ura3</i> $\Delta$ <i>FRT-YKU80</i> <i>atg32</i> $\Delta$ :: <i>HIS3</i>	This study
<i>Cgatg1</i> $\Delta$ - <i>mtDHFR-GFP</i>	<i>trp1</i> $\Delta$ <i>his3</i> $\Delta$ :: <i>GPD</i> <sup>P</sup> - <i>mito-mouse DHFR-GFP</i> <i>ura3</i> $\Delta$ <i>FRT-YKU80</i> <i>atg1</i> $\Delta$ :: <i>HIS3</i>	This study
<i>Cgatg11</i> $\Delta$ - <i>mtDHFR-GFP</i>	<i>trp1</i> $\Delta$ <i>his3</i> $\Delta$ :: <i>GPD</i> <sup>P</sup> - <i>mito-mouse DHFR-GFP</i> <i>ura3</i> $\Delta$ <i>FRT-YKU80</i> <i>atg11</i> $\Delta$ :: <i>HIS3</i>	This study
BY4741	<i>MATa his3</i> $\Delta$ 1 <i>leu2</i> $\Delta$ 0 <i>met15</i> $\Delta$ 0 <i>ura3</i> $\Delta$ 0	43
BYmtDHFR-GFP	BY4741 [p416GPD- <i>mtDHFR-GFP</i> ]	This study
Plasmid	Feature	Reference
p416GPD- <i>mtDHFR-GFP</i>	<i>CEN URA3 GPD</i> <sup>P</sup> <i>N. crassa</i> <i>ATP9</i> (1-69) + mouse <i>DHFR</i> + <i>brighterGFP</i>	8
pHIS906	Carrying <i>CgHIS3</i> marker, PCR template for the cassette amplification	42
pTi-comp	Carrying <i>CgTRP1</i> marker, PCR template for the cassette amplification	48

<sup>a</sup> The indicated genes refer to *C. glabrata* unless otherwise noted. *Sc*; *Saccharomyces cerevisiae*.

### Reintroduction of CgATG32 into Cgatg32Δ mutants

DNA fragments harboring the CgATG32 ORF were amplified from the CBS138 genome using the primers ATG32 compF/-1kb and ATG32 compR/1979r. The amplified fragment containing the CgATG32 ORF was digested with BamHI and XhoI, which yielded a DNA fragment that was cloned into the BamHI and Sall sites of pTi-comp.<sup>44</sup> Using these plasmids as the template, insertion fragments were amplified using the primers ATG32-Rev-F and ATG32-Rev-R. The resulting DNA fragment was introduced into the CgHIS3 gene-replaced locus in the CgATG32 deletant chromosome by end-in type recombination.<sup>45</sup> Accurate insertion of the amplified fragment into the correct chromosomal locus was confirmed by PCR using the primers ATG32 up -1050 to -1031 and ATG32 ORF 20-1. The sequences of all the primers are listed in Table S2. Integration of DNA fragment into the designated locus was also confirmed by Southern blot analysis (Fig. S1).

### Southern blot analysis

Southern blot analysis was performed as described previously.<sup>46</sup> All of the restriction enzymes used in the experiments are shown in Figure S1. The probe, which corresponded to nucleotides 200–480 or 44–606 relative to the start codon of CgHIS3 or CgTRP1, was amplified with the oligonucleotides HIS3f and HIS3r, or TRP1f and TRP1r, respectively (Table S2).

### Semi-quantitative RT-PCR

Semi-quantitative RT-PCR was performed as described previously.<sup>46</sup> All of the primers used for qRT-PCR are listed in Table S2. All experiments were repeated based on 3 independent preparations of RNA and the mean ± SEM represented the results of 3 experiments.

### Detection of mitophagy by western blotting

Detection of mitophagy was conducted according to previously described methods.<sup>47</sup> *C. glabrata* cells expressing mtDHFR-GFP were cultured in 1 mL of YPD medium overnight. These cells were collected by centrifugation and washed with sterile water, inoculated at approximately  $3 \times 10^5$  cells/mL, and cultured in 5 mL of medium. The incubated cells were harvested at specific time points and the optical density at 600 nm ( $OD_{600}$ ) was estimated. Cell aliquots equivalent to 1  $OD_{600}$  unit were placed in 1.5 mL microcentrifuge tubes. Trichloroacetic acid (10% final concentration) was added to the samples, which were then incubated for 10 min on ice. The proteins were pelleted by centrifugation at  $21,000 \times g$  for 10 min. After washing the pellet fraction twice with 1 mL of ice-cold acetone, the pellet was air dried. The air-dried cell pellet was resuspended in 50  $\mu$ L of sample buffer (150 mM Tris-HCl, pH 8.8, 6% SDS [Wako Pure Chemical Industries, Ltd., 191-07145], 25% glycerol, 6 mM EDTA, 0.5% 2-mercaptoethanol, 0.05% bromophenol blue) and disrupted by vortexing with an equal volume of acid-washed glass beads for 3 min. The samples were then incubated at 100°C for 3 min. Next, 3  $\mu$ L aliquots of the samples were loaded onto a 12.5% polyacrylamide gel and resolved. A

standard semi-dry western blot transfer procedure was performed using PVDF membranes. After blotting, the membranes were probed with anti-GFP antibody (1:25,000 dilution; Clontech, 632380) by incubating for 1 h at room temperature. After washing the membranes 3 times each for 10 min in Tris-buffered saline containing Tween 20 (TTBS; 50 mM Tris-HCl, pH 7.6, 0.9% NaCl, 0.1% Tween 20 [Sigma-Aldrich, P9416]), a secondary incubation was performed with HRP-conjugated anti-mouse IgG (1:20,000 dilution; Thermo Fisher Scientific, 32430) for 1 h at room temperature. After washing the membrane 3 times each for 10 min in TTBS, the GFP signal was detected using an ECL kit (Wako Pure Chemical Industries, Ltd., 296-69901). Quantification of the fluorescence intensity was performed using a C-DiGit Blot Scanner and ImageStudio software (LI-COR Biosciences, Lincoln, NE). MtDHFR-GFP and processed GFP were detected as bands that migrated at molecular masses of approximately 50 and 28 kDa, respectively.

### Lambda protein phosphatase ( $\lambda$ PP) treatment

*C. glabrata* cells expressing HA-CgATG32 were cultured in 1 mL of YPD medium overnight. These cells were collected by centrifugation and washed twice with sterile water, inoculated at approximately  $3 \times 10^5$  cells/mL, and cultured in 50 mL of SD or SD-Fe medium. The incubated cells were harvested at specific time points and the optical density at 600 nm ( $OD_{600}$ ) was estimated. Cell aliquots equivalent to 30  $OD_{600}$  unit were placed in 2.0 mL homogenizing tubes (Yasui kikai Co., ST-0250). These cells were collected by centrifugation and washed twice with ice-cold sterile water. The following procedures were performed on ice or at 4 °C: The cells were suspended in 700  $\mu$ L of homogenizing buffer (50 mM Tris-HCl, pH 7.5, 2 mM EDTA, 1 mM phenylmethanesulfonyl fluoride [PMSF; Roche Applied Science, 1873636]), and 700 mg of glass beads (Sigma-Aldrich, G8772) were added to the cell suspension. The cells were disrupted using a Multi-beads shocker (Yasui Kikai Co., MB1001C[S]) at 2,700 rpm for 5 min. The cell extract was collected, and the glass beads were washed with up to 1 mL of homogenizing buffer containing 1 mM PMSF. The cell extract was centrifuged ( $2,000 \times g$  for 10 min) to remove unbroken cells and cellular debris, and the supernatant fraction was centrifuged at  $20,000 \times g$  for 45 min. The pellet was washed with 500  $\mu$ L of NEBuffer for PMP (50 mM HEPES, 100 mM NaCl, 2 mM DTT, 0.01% Brij 35 [New England Biolabs, P0753S], pH 7.5) and centrifuged at  $20,000 \times g$  for 45 min. The pellet was resuspended in 50  $\mu$ L of NEBuffer for PMP with 1.5  $\mu$ L of  $\lambda$  PP (+; NEB, 400,000 U/ml) and without  $\lambda$  PP (-), incubated at 30°C for 1 h and centrifuged at  $20,000 \times g$  for 45 min. The pellet fraction was resuspended in 30  $\mu$ L of sample buffer and incubated at 100°C for 3 min. The protein concentrations of these samples were determined by a Bradford Protein Assay (APRO SCIENCE, KY-1030) with bovine serum albumin as the standard. Next, 20  $\mu$ g aliquots of the samples were loaded onto a 10% polyacrylamide gel and resolved. A standard semi-dry western blot transfer procedure was performed as described above. Primary antibody treatment was performed using anti-HA antibody (F-7, 1:1,000 dilution; Santa Cruz Biotechnology, sc-7392).

### Anaerobic incubation

Anaerobic conditions were obtained with an anaerobic rectangular jar and Anaero pack-Anaero (Mitsubishi Gas Chemical Company, inc., A-41). *C. glabrata* strains were inoculated from an overnight saturated YPD culture to  $OD_{600} = 0.002$  in 75 mL Flask with Vent Cap (Corning, 430641) with 30 mL SD medium at 30°C in the anaerobic jar with Anaero pack-Anaero.

### CLS assay

Overnight cultures in 1 mL of YPD medium (starting from single isolated colonies) were diluted to 0.1  $OD_{600}$  units in 10 mL of medium and incubated at 30°C with shaking at 200 rpm. Viability was measured by plating aging cells onto YPD agar plates and monitoring the CFU levels at specific time points. The initial viability was defined as 100%. The experiment was performed in triplicate.

### Detection of protein oxidation level

Protein samples were prepared as described above for the western blotting analyses. The protein oxidization levels were determined using an OxyBlot™ Protein Oxidation Detection kit (Millipore, S7150), according to the manufacturer's instructions.

### Measurements of cellular ROS level and MMP

Overnight cultures in 1 mL of YPD medium (starting from single isolated colonies) were diluted to 0.1  $OD_{600}$  unit in 10 mL of medium and incubated at 30°C with shaking at 200 rpm. The cells were collected by centrifugation and incubated in PBS with 15  $\mu$ M DHE (Sigma-Aldrich, D7008) to measure the cellular ROS level or 175 nM DiOC<sub>6</sub>(3) (Thermo Fisher Scientific, D-273) to measure the MMP, for 30 min at 30°C with shaking at 200 rpm. Stained cells were washed and resuspended in PBS, and then analyzed using a fluorescence-activated cell sorter (BD FACSCalibur; BD Biosciences). The obtained data were analyzed using FlowJo software (Tree Star). The following parameters were used: FL1 for DiOC<sub>6</sub>(3), FL2 for DHE, side scatter, and forward scatter. The experiment was performed in triplicate ( $n = 3$ ) and 30,000 events were registered for each sample. Statistical analyses were performed using GraphPad Prism6™ (GraphPad Software) via an unpaired *t* test with a significance level of  $P < 0.05$ .

### Animal studies

The tissue fungal burden and expression analysis were performed as described previously.<sup>46</sup> The male BALB/c mice 7 wk of age (Japan SLC, Inc.) and the male CD-1 mice 4 wk of age (Charles River Laboratories Japan, Inc.) were used for evaluation of the fungal burden and the gene expression, respectively. CD-1 mice were rendered neutropenic by intraperitoneal administration of cyclophosphamide and cortisone acetate. The mice were injected into their tail vein with saline suspensions of a *C. glabrata* strain (in a volume of 200  $\mu$ L). After seven days, mice were sacrificed, and target organs (kidney and spleen) were excised aseptically. Organ homogenates were diluted and plated onto YPD containing streptomycin sulfate

(Sigma-Aldrich) and penicillin G sodium salt (Sigma-Aldrich). Colonies were counted after a day of incubation at 37°C, and the numbers of CFU/g of organ were calculated. In the case of CD-1 mice, *C. glabrata* colonies on kidney were collected, and used for gene expression analysis as described above. Statistical analyses were performed using GraphPad Prism6™ via an unpaired *t* test with a significance level of  $P < 0.05$ . Primers used for the expression analysis are listed in Table S2.

### Abbreviations

CFU	colony-forming unit
CLS	chronological life span
DHE	dihydroethidium
DHFR	dihydrofolate reductase
DiOC <sub>6</sub> (3)	3,3'-dihexyloxycarbocyanine iodide
ECL	enhanced chemiluminescence
GFP	green fluorescent protein
GSH	glutathione
HA	hemagglutinin
MMP	mitochondrial membrane potential
NAC	N-acetyl-L-cysteine
OD	optical density
PMSF	phenylmethane sulfonyl fluoride
ROS	reactive oxygen species
RT-PCR	reverse transcription-polymerase chain reaction
SD	synthetic glucose medium
SEM	standard error of the mean
TTBS	Tris-buffered saline containing Tween 20
WT	wild type
YPD	yeast extract peptone dextrose
$\lambda$ PP	lambda protein phosphatase

### Disclosure of potential conflicts of interest

No potential conflicts of interest were disclosed.

### Acknowledgments

We thank Koji and Noriko Okamoto (Graduate School of Frontier Biosciences, Osaka University, Suita, Osaka 565-0871, Japan) for providing yeast strains and plasmids. This research was supported by JSPS KAKENHI Grant Numbers 26790428 (KT), 24590540 (HN), and 26860296 (MN). This work was partly supported by a grant from the Ministry of Health, Labor and Welfare of Japan (H26-shinkoujitsuyouka-ippan-010). The authors would like to thank Enago (<http://www.enago.jp>) for the English language review.

### References

- [1] Miceli MH, Díaz JA, Lee SA. Emerging opportunistic yeast infections. *Lancet Infect Dis* 2011; 11:142-51; PMID:21272794; [http://dx.doi.org/10.1016/S1473-3099\(10\)70218-8](http://dx.doi.org/10.1016/S1473-3099(10)70218-8)
- [2] Roetzer A, Gabaldón T, Schüller C. From *Saccharomyces cerevisiae* to *Candida glabrata* in a few easy steps: important adaptations for an opportunistic pathogen. *FEMS Microbiol Lett* 2011; 314:1-9; PMID:20846362; <http://dx.doi.org/10.1111/j.1574-6968.2010.02102.x>
- [3] Turrens JF. Mitochondrial formation of reactive oxygen species. *J Physiol* 2003; 552:335-44; PMID:14561818; <http://dx.doi.org/10.1113/jphysiol.2003.049478>

- [4] Kurihara Y, Kanki T, Aoki Y, Hirota Y, Saigusa T, Uchiyumi T, Kang D. Mitophagy plays an essential role in reducing mitochondrial production of reactive oxygen species and mutation of mitochondrial DNA by maintaining mitochondrial quantity and quality in yeast. *J Biol Chem* 2012; 287:3265-72; PMID:22157017; <http://dx.doi.org/10.1074/jbc.M111.280156>
- [5] Narendra DP, Jin SM, Tanaka A, Suen D-F, Gautier C a, Shen J, Cookson MR, Youle RJ. PINK1 is selectively stabilized on impaired mitochondria to activate Parkin. *PLoS Biol* 2010; 8:e1000298; PMID:20126261; <http://dx.doi.org/10.1371/journal.pbio.1000298>
- [6] Narendra D, Tanaka A, Suen D-F, Youle RJ. Parkin is recruited selectively to impaired mitochondria and promotes their autophagy. *J Cell Biol* 2008; 183:795-803; PMID:19029340; <http://dx.doi.org/10.1083/jcb.200809125>
- [7] Kanki T, Wang K, Cao Y, Baba M, Klionsky DJ. Atg32 is a mitochondrial protein that confers selectivity during mitophagy. *Dev Cell* 2009; 17:98-109; PMID:19619495; <http://dx.doi.org/10.1016/j.devcel.2009.06.014>
- [8] Okamoto K, Kondo-Okamoto N, Ohsumi Y. Mitochondria-anchored receptor Atg32 mediates degradation of mitochondria via selective autophagy. *Dev Cell* 2009; 17:87-97; PMID:19619494; <http://dx.doi.org/10.1016/j.devcel.2009.06.013>
- [9] Kanki T, Wang K, Baba M, Bartholomew CR, Lynch-Day MA, Du Z, Geng J, Mao K, Yang Z, Yen W-L, et al. A genomic screen for yeast mutants defective in selective mitochondria autophagy. *Mol Biol Cell* 2009; 20:4730-8; PMID:19793921; <http://dx.doi.org/10.1091/mbc.E09-03-0225>
- [10] Kanki T, Klionsky DJ. Mitophagy in yeast occurs through a selective mechanism. *J Biol Chem* 2008; 283:32386-93; PMID:18818209; <http://dx.doi.org/10.1074/jbc.M802403200>
- [11] Richard VR, Leonov A, Beach A, Burstein MT, Koupaki O, Gomez-Perez A, Levy S, Pluska L, Mattie S, Rafesh R, et al. Macromitophagy is a longevity assurance process that in chronologically aging yeast limited in calorie supply sustains functional mitochondria and maintains cellular lipid homeostasis. *Aging* 2013; 5:234-69; PMID:23553280; <http://dx.doi.org/10.18632/aging.100547>
- [12] Mesquita A, Weinberger M, Silva A, Sampaio-Marques B, Almeida B, Leão C, Costa V, Rodrigues F, Burhans WC, Ludovico P. Caloric restriction or catalase inactivation extends yeast chronological lifespan by inducing H<sub>2</sub>O<sub>2</sub> and superoxide dismutase activity. *Proc Natl Acad Sci U S A* 2010; 107:15123-8; PMID:20696905; <http://dx.doi.org/10.1073/pnas.1004432107>
- [13] Smith DL, McClure JM, Matecic M, Smith JS. Calorie restriction extends the chronological lifespan of *Saccharomyces cerevisiae* independently of the Sirtuins. *Aging Cell* 2007; 6:649-62; PMID:17711561; <http://dx.doi.org/10.1111/j.1474-9726.2007.00326.x>
- [14] Lin S-J. Requirement of NAD and SIR2 for Life-Span Extension by Calorie Restriction in *Saccharomyces cerevisiae*. *Science* 2000; 289:2126-8; PMID:11000115; <http://dx.doi.org/10.1126/science.289.5487.2126>
- [15] Choi J-S, Lee C-K. Maintenance of cellular ATP level by caloric restriction correlates chronological survival of budding yeast. *Biochem Biophys Res Commun* 2013; 439:126-31; PMID:23942118; <http://dx.doi.org/10.1016/j.bbrc.2013.08.014>
- [16] Agarwal S, Sharma S, Agrawal V, Roy N. Caloric restriction augments ROS defense in *S. cerevisiae*, by a Sir2p independent mechanism. *Free Radic Res* 2005; 39:55-62; PMID:15875812; <http://dx.doi.org/10.1080/10715760400022343>
- [17] Sasaki K, Ikuta K, Tanaka H, Ohtake T, Torimoto Y, Fujiya M, Kohgo Y. Improved quantification for non-transferrin-bound iron measurement using high-performance liquid chromatography by reducing iron contamination. *Mol Med Rep* 2011; 4:913-8; PMID:21720715
- [18] Sutak R, Lesuisse E, Tachezy J, Richardson DR. Crusade for iron: iron uptake in unicellular eukaryotes and its significance for virulence. *Trends Microbiol* 2008; 16:261-8; PMID:18467097; <http://dx.doi.org/10.1016/j.tim.2008.03.005>
- [19] Nevitt T, Thiele DJ. Host iron withholding demands siderophore utilization for *Candida glabrata* to survive macrophage killing. *PLoS Pathog* 2011; 7:e1001322; PMID:21445236; <http://dx.doi.org/10.1371/journal.ppat.1001322>
- [20] Aihara M, Jin X, Kurihara Y, Yoshida Y, Matsushima Y, Oku M, Hirota Y, Saigusa T, Aoki Y, Uchiyumi T, et al. Tor and the Sin3-Rpd3 complex regulate expression of the mitophagy receptor protein Atg32 in yeast. *J Cell Sci* 2014; 127:3184-96; PMID:24838945; <http://dx.doi.org/10.1242/jcs.153254>
- [21] Aoki Y, Kanki T, Hirota Y, Kurihara Y, Saigusa T, Uchiyumi T, Kang D. Phosphorylation of Serine 114 on Atg32 mediates mitophagy. *Mol Biol Cell* 2011; 22:3206-17; PMID:21757540; <http://dx.doi.org/10.1091/mbc.E11-02-0145>
- [22] Mao K, Wang K, Zhao M, Xu T, Klionsky DJ. Two MAPK-signaling pathways are required for mitophagy in *Saccharomyces cerevisiae*. *J Cell Biol* 2011; 193:755-67; PMID:21576396; <http://dx.doi.org/10.1083/jcb.201102092>
- [23] Straub M, Bredschneider M, Thumm M. *AUT3*, a serine/threonine kinase gene, is essential for autophagocytosis in *Saccharomyces cerevisiae*. *J Bacteriol* 1997; 179:3875-83; PMID:9190802
- [24] Kamada Y, Funakoshi T, Shintani T, Nagano K, Ohsumi M, Ohsumi Y. Tor-mediated induction of autophagy via an Apg1 protein kinase complex. *J Cell Biol* 2000; 150:1507-13; PMID:10995454; <http://dx.doi.org/10.1083/jcb.150.6.1507>
- [25] Puig S, Askeland E, Thiele DJ. Coordinated remodeling of cellular metabolism during iron deficiency through targeted mRNA degradation. *Cell* 2005; 120:99-110; PMID:15652485; <http://dx.doi.org/10.1016/j.cell.2004.11.032>
- [26] Shakoury-Elizeh M, Protchenko O, Berger A, Cox J, Gable K, Dunn TM, Prinz WA, Bard M, Philpott CC. Metabolic response to iron deficiency in *Saccharomyces cerevisiae*. *J Biol Chem* 2010; 285:14823-33; PMID:20231268; <http://dx.doi.org/10.1074/jbc.M109.091710>
- [27] Raymond KN, Dertz EA, Kim SS. Enterobactin: an archetype for microbial iron transport. *Proc Natl Acad Sci U S A* 2003; 100:3584-8; PMID:12655062; <http://dx.doi.org/10.1073/pnas.0630018100>
- [28] Dujon B, Sherman D, Fischer G, Durrrens P, Casaregola S, Lafontaine I, De Montigny J, Marck C, Neuvéglise C, Talla E, et al. Genome evolution in yeasts. *Nature* 2004; 430:35-44; PMID:15229592; <http://dx.doi.org/10.1038/nature02579>
- [29] Kaur R, Domergue R, Zupancic ML, Cormack BP. A yeast by any other name: *Candida glabrata* and its interaction with the host. *Curr Opin Microbiol* 2005; 8:378-84; PMID:15996895; <http://dx.doi.org/10.1016/j.mib.2005.06.012>
- [30] Ehrlich GD, Hiller NL, Hu FZ. What makes pathogens pathogenic. *Genome Biol* 2008; 9:225; PMID:18598378; <http://dx.doi.org/10.1186/gb-2008-9-6-225>
- [31] Allen GFG, Toth R, James J, Ganley IG. Loss of iron triggers PINK1/Parkin-independent mitophagy. *EMBO Rep* 2013; 14:1127-35; PMID:24176932; <http://dx.doi.org/10.1038/embor.2013.168>
- [32] Harris N, Costa V, MacLean M, Mollapour M, Moradas-Ferreira P, Piper PW. Mnsod overexpression extends the yeast chronological (G (0)) life span but acts independently of Sir2p histone deacetylase to shorten the replicative life span of dividing cells. *Free Radic Biol Med* 2003; 34:1599-606; PMID:12788479; [http://dx.doi.org/10.1016/S0891-5849\(03\)00210-7](http://dx.doi.org/10.1016/S0891-5849(03)00210-7)
- [33] Longo VD. Mutations in signal transduction proteins increase stress resistance and longevity in yeast, nematodes, fruit flies, and mammalian neuronal cells. *Neurobiol Aging* 1999; 20:479-86; PMID:10638521; [http://dx.doi.org/10.1016/S0197-4580\(99\)00089-5](http://dx.doi.org/10.1016/S0197-4580(99)00089-5)
- [34] Unlu ES, Koc A. Effects of deleting mitochondrial antioxidant genes on life span. *Ann N Y Acad Sci* 2007; 1100:505-9; PMID:17460215; <http://dx.doi.org/10.1196/annals.1395.055>
- [35] Giancaspero TA, Dipalo E, Miccolis A, Boles E, Caselle M, Barile M. Alteration of ROS Homeostasis and Decreased Lifespan in *S. cerevisiae* Elicited by Deletion of the Mitochondrial Translocator *FLX1*. *Biomed Res Int* 2014; 2014; PMID: 24895546; <http://dx.doi.org/10.1155/2014/101286>
- [36] Pan Y, Schroeder EA, Ocampo A, Barrientos A, Shadel GS. Regulation of yeast chronological life span by TORC1 via adaptive mitochondrial ROS signaling. *Cell Metab* 2011; 13:668-78; PMID:21641548; <http://dx.doi.org/10.1016/j.cmet.2011.03.018>

- [37] Lai C-Y, Jaruga E, Borghouts C, Jazwinski SM. A mutation in the *ATP2* gene abrogates the age asymmetry between mother and daughter cells of the yeast *Saccharomyces cerevisiae*. *Genetics* 2002; 162:73-87; PMID:12242224
- [38] Borghouts C, Benguria A, Wawryn J, Jazwinski SM. Rtg2 protein links metabolism and genome stability in yeast longevity. *Genetics* 2004; 166:765-77; PMID:15020466; <http://dx.doi.org/10.1534/genetics.166.2.765>
- [39] Barros MH, Bandy B, Tahara EB, Kowaltowski AJ. Higher respiratory activity decreases mitochondrial reactive oxygen release and increases life span in *Saccharomyces cerevisiae*. *J Biol Chem* 2004; 279:49883-8; PMID:15383542; <http://dx.doi.org/10.1074/jbc.M408918200>
- [40] Deffieu M, Bhatia-Kissová I, Salin B, Galinier A, Manon S, Camougrand N. Glutathione participates in the regulation of mitophagy in yeast. *J Biol Chem* 2009; 284:14828-37; PMID:19366696; <http://dx.doi.org/10.1074/jbc.M109.005181>
- [41] Sjödin K, Nilsson E, Hallberg A, Tunek A. Metabolism of N-acetyl-L-cysteine. Some structural requirements for the deacetylation and consequences for the oral bioavailability. *Biochem Pharmacol* 1989; 38:3981-5; PMID:2597179; [http://dx.doi.org/10.1016/0006-2952\(89\)90677-1](http://dx.doi.org/10.1016/0006-2952(89)90677-1)
- [42] Ueno K, Uno J, Nakayama H, Sasamoto K, Mikami Y, Chibana H. Development of a highly efficient gene targeting system induced by transient repression of *YKU80* expression in *Candida glabrata*. *Eukaryot Cell* 2007; 6:1239-47; PMID:17513567; <http://dx.doi.org/10.1128/EC.00414-06>
- [43] Brachmann CB, Davies A, Cost GJ, Caputo E, Li J, Hieter P, Boeke JD. Designer deletion strains derived from *Saccharomyces cerevisiae* S288C: a useful set of strains and plasmids for PCR-mediated gene disruption and other applications. *Yeast* 1998; 14:115-32; PMID:9483801; [http://dx.doi.org/10.1002/\(SICI\)1097-0061\(19980130\)14:2%3c115::AID-YEA204%3e3.0.CO;2-2](http://dx.doi.org/10.1002/(SICI)1097-0061(19980130)14:2%3c115::AID-YEA204%3e3.0.CO;2-2)
- [44] Kitada K, Yamaguchi E, Arisawa M. Isolation of a *Candida glabrata* centromere and its use in construction of plasmid vectors. *Gene* 1996; 175:105-8; PMID:8917084; [http://dx.doi.org/10.1016/0378-1119\(96\)00132-1](http://dx.doi.org/10.1016/0378-1119(96)00132-1)
- [45] Yamana Y, Maeda T, Ohba H, Usui T, Ogawa HI, Kusano K. Regulation of homologous integration in yeast by the DNA repair proteins Ku70 and RecQ. *Mol Genet Genomics* 2005; 273:167-76; PMID:15803320; <http://dx.doi.org/10.1007/s00438-005-1108-y>
- [46] Nagi M, Tanabe K, Ueno K, Nakayama H, Aoyama T, Chibana H, Yamagoe S, Umeyama T, Oura T, Ohno H, et al. The *Candida glabrata* sterol scavenging mechanism, mediated by the ATP-binding cassette transporter Aus1p, is regulated by iron limitation. *Mol Microbiol* 2013; 88:371-81; PMID:23448689; <http://dx.doi.org/10.1111/mmi.12189>
- [47] Kanki T, Kang D, Klionsky DJ. Monitoring mitophagy in yeast: the Om45-GFP processing assay. *Autophagy* 2009; 5:1186-9; PMID:19806021; <http://dx.doi.org/10.4161/auto.5.8.9854>
- [48] Nagi M, Nakayama H, Tanabe K, Bard M, Aoyama T, Okano M, Higashi S, Ueno K, Chibana H, Niimi M, Yamagoe S, Umeyama T, Kajiwara S, Ohno H, Miyazaki Y. Transcription factors *CgUPC2A* and *CgUPC2B* regulate ergosterol biosynthetic genes in *Candida glabrata*. *Genes Cells* 2011; 16:80-9; PMID:21199190; <http://dx.doi.org/10.1111/j.1365-2443.2010.01470.x>